Mechanism of Ivermectin Facilitation of Human $P2X_4$ Receptor Channels

Avi Priel and Shai D. Silberberg

Department of Life Sciences and The Zlotowski Center for Neuroscience, Ben-Gurion University of the Negev, Beer-Sheva 84105, Israel

ABSTRACT Ivermectin (IVM), a widely used antiparasitic agent in human and veterinary medicine, was recently shown to augment macroscopic currents through rat $P2X_4$ receptor channels (Khakh, B.S., W.R. Proctor, T.V. Dunwiddie, C. Labarca, and H.A. Lester. 1999. *J. Neurosci.* 19:7289–7299.). In the present study, the effects of IVM on the human $P2X_4$ ($hP2X_4$) receptor channel stably transfected in HEK293 cells were investigated by recording membrane currents using the patch clamp technique. In whole-cell recordings, IVM (≤10 μM) applied from outside the cell (but not from inside) increased the maximum current activated by ATP, and slowed the rate of current deactivation. These two phenomena likely result from the binding of IVM to separate sites. A higher affinity site (EC_{50} 0.25 μM) increased the maximal current activated by saturating concentrations of ATP without significantly changing the rate of current deactivation or the EC_{50} and Hill slope of the ATP concentration-response relationship. A lower affinity site (EC_{50} 2 μM) slowed the rate of current deactivation, and increased the apparent affinity for ATP. In cell-attached patch recordings, $P2X_4$ receptor channels exhibited complex kinetics, with multiple components in both the open and shut distributions. IVM (0.3 μM) increased the number of openings per burst, without significantly changing the mean open or mean shut time within a burst. At higher concentrations (1.5 μM) of IVM, two additional open time components of long duration were observed that gave rise to long-lasting bursts of channel activity. Together, the results suggest that the binding of IVM to the higher affinity site increases current amplitude by reducing channel desensitization, whereas the binding of IVM to the lower affinity site slows the deactivation of the current predominantly by stabilizing the open conformation of the channel.

KEY WORDS: ion channel gating • allosteric regulation • purinergic receptors • ATP • patch clamp techniques

INTRODUCTION

Ivermectin (IVM), a semisynthetic derivative of the natural fermentation products of *Streptomyces avermitilis* (Fig. 1 A), is widely used in human and veterinary medicine as an antiparasitic agent (Burkhart, 2000). In humans, more than 18 million people receive IVM annually, predominantly to treat onchoceriasis (river blindness). Experiments on model organisms strongly suggest that at therapeutic levels, IVM activates glutamate-gated chloride channels in the nerves and muscles of the parasite, leading to membrane hyperpolarization and muscle paralysis (Dent et al., 1997, 2000). Thus, the major mode of action of IVM is most likely the disruption of ingestive activity of the parasite, resulting in starvation. An IVM-sensitive glutamate-gated chloride channel was first cloned from *Caenorhabditis elegans* using expression cloning (Cully et al., 1994). Two cDNA clones (GluCl α and GluCl β) were isolated that form functional homomeric and heteromeric channels. Interestingly, the binding site for IVM was on the α subunit while the binding site for glutamate was on the β subunit. In channels containing both subunits, IVM directly activated the channels at high concentrations and at low concentrations potentiated the response to glutamate. Thus, IVM is both an agonist and an allosteric modulator of glutamate gated chloride channels. Subsequently, a glutamate-gated chloride channel subunit was cloned that forms homomeric glutamate and IVM-sensitive channels (Dent et al., 1997; Vassilatis et al., 1997). The three *C. elegans* genes encoding the glutamate-gated chloride channel subunits collectively account for the sensitivity of the nematode to IVM (for review see Burkhart, 2000; Dent et al., 2000; Köhler, 2001).

Several other ligand-gated ion channels are activated and/or modulated by IVM. These include a crayfish multiagonist–gated chloride-selective channel (Zufall et al., 1989); $GABA_A$ receptors from nematode (Feng et al., 2002), chick (Sigel and Baur, 1987), mouse (Krusek and Zemková, 1994), rat (Adelsberger et al., 2000), and human (Dawson et al., 2000); α7 nicotinic receptors from chick and human (Krause et al., 1998), human glycine receptor (Shan et al., 2001), the histamine receptor from fly (Zheng et al., 2002), and the $P2X_4$ receptor channel from rat (Khakh et al., 1999; Bowler et

Address correspondence to Shai Silberberg, Department of Life Sciences Ben-Gurion, University of the Negev, P.O. Box 653, Beer-Sheva 84105, Israel. Fax: (972) 8-6461-710; email: Silber@bgumail.bgu.ac.il

Abbreviation used in this paper: IVM, ivermectin.

al., 2003). This seeming nonspecific nature of IVM action on ligand-gated channels is misleading since several instances of specificity exist. For example, $P2X_2$, $P2X_3$, and $P2X_7$ receptor channels, which are homologous to the $P2X_4$ receptor channel, are not modulated by IVM, indicating that specific structural requirements most likely exist for IVM action.

P2X receptors are cation-selective channels gated by extracellular ATP (North, 2002). Of the seven cloned subunits ($P2X_1$–$P2X_7$), all but $P2X_6$ can form functional homomeric cation-selective channels. As mentioned above, Khakh et al. (1999) investigated the effects of IVM on homomeric rat $P2X_2$, $P2X_3$, $P2X_4$, and $P2X_7$ receptor channels expressed in *Xenopus* oocytes using the double-electrode voltage-clamp technique and found only $P2X_4$ to be sensitive to IVM. IVM alone did not directly activate the $P2X_4$ receptor channels, but preincubating the oocytes with 0.1–10 μM IVM had dramatic effects on the current activated by ATP. IVM increased the maximal current activated by saturating ATP concentrations and slowed the rate of current deactivation after the washout of ATP. In addition, IVM increased the potency of ATP and of the weak agonist α,β-methylene-ATP. Together, these results indicate that IVM is an allosteric modulator of rat $P2X_4$ receptors, but do not reveal the mechanisms by which IVM modulates the channels.

To better understand the molecular effects of IVM on $P2X_4$ receptor channels, we examined the changes induced by IVM to whole-cell and single-channel currents of the human $P2X_4$ ($hP2X_4$) receptor channel expressed in HEK293 cells. We found that IVM likely binds to separate extracellular sites on the $hP2X_4$ receptor channel to modulate current amplitude and the rate of current deactivation. At low concentrations IVM predominantly augments the maximal current activated by ATP, while higher concentrations of IVM predominantly slow the rate of current deactivation and increase the potency of ATP. The single-channel data suggest that IVM increases current amplitude by reducing channel desensitization, while the slowing of current deactivation results primarily from the stabilization of an open conformation of the channel.

MATERIALS AND METHODS

Materials

Solutions for electrophysiology were made with highly purified water (NANOpure) using chemicals of analytical grade. ATP (potassium salt) and IVM were purchased from Sigma-Aldrich. Solutions containing ATP were prepared freshly each day and the pH of the solution was readjusted. IVM was dissolved in DMSO (Sigma-Aldrich); the stock solutions were kept at −20°C for 2 wk. The concentration of DMSO in the final solutions did not exceed 0.03%.

Cell Culture

Human embryonic kidney cells (HEK293) stably transfected with human $P2X_4$ (provided by Dr. Soto and Dr. Stühmer) were grown in DMEM/F12 supplemented with 10% fetal calf serum, 100 units ml^{-1} penicillin, 100 mg ml^{-1} streptomycin, and 0.5 mg/ml geneticin (G-418) in a 37°C incubator with 95% air and 5% CO_2. When the cultures were 70–90% confluent, the cells were mechanically dispersed and plated on 9-mm coverslips in 35-mm culture dishes, and used for recording within 1–3 d. Cells were used up to passage 15. All cell-culture chemicals were purchased from GIBCO BRL.

Whole-cell Current Recording

Membrane currents were recorded using the standard whole-cell configuration of the patch-clamp technique (Sakmann and Neher, 1995). Once the whole-cell configuration was established, the cell was continuously superfused with extracellular solutions via a computer-controlled rapid perfusion system (RSC-200; Bio-logic). Experiments were initiated at least 2 min after establishing the whole-cell configuration to allow equilibration of the cytosol with the pipette solution. Membrane currents were recorded under voltage-clamp using an Axopatch 200A patch-clamp amplifier (Axon Instruments, Inc.) and stored on VCR tape for subsequent analysis (VR-10B; Instrutech). Membrane currents were also digitized on-line using a Digidata 1200 interface board and pCLAMP 6.03 software (Axon Instruments, Inc.). The sampling frequency was set to at least two times the corner frequency of the low-pass filter. The standard extracellular solution contained (mM): 140 NaCl, 5.4 KCl, 0.5 $MgCl_2$, 2 $CaCl_2$, 10 HEPES, and 10 D-glucose, adjusted to pH 7.4 with NaOH, 315–320 mOsmol Kg^{-1}. The standard pipette solution contained (mM): 140 KCl, 2 $MgCl_2$, 2 TEA-Cl, 11 EGTA, 10 HEPES, adjusted to pH 7.2 with KOH, 330 mOsmol Kg^{-1}.

Whole-cell perforated-patch current recordings were performed as previously described (Horn and Marty, 1988; Silberberg and van Breemen, 1992). A 100-mg/ml stock of nystatin was prepared fresh every 2 h in DMSO, and diluted 1:1,000 with pipette solution containing (mM): 75 K_2SO_4, 55 KCl, 5 $MgSO_4$, and 10 HEPES, adjust to pH 7.2 with KOH, 310–315 mOsmol Kg^{-1}. The extracellular solution contained (mM): 160 NaCl, 2 $CaCl_2$, and 10 HEPES, adjust to pH 7.4 with NaOH, 330 mOsmol Kg^{-1}. Only cells that had a series resistance of <15 MΩ were analyzed.

Single-channel Current Recording

Single-channel currents were recorded in either the outside-out patch configuration or the on-cell (cell-attached) configuration of the patch-clamp technique (Hamill et al., 1981). For the outside-out recordings, the dissociated cells were anchored to the bottom of the experimental chamber using glass coverslips coated with concanavalin A (Sigma-Aldrich), as described by Kim et al. (1993). The external solution contained (mM): 147 NaCl, 1 $CaCl_2$, 10 HEPES, and 11 D-glucose, adjust to pH 7.4 with NaOH, 320 mOsmol Kg^{-1}. Several different concentrations of Ca^{2+} (between nominally Ca^{2+} free and 2 mM) were tested in the outside-out and cell-attached configurations, as Ca^{2+} has been shown to block $P2X_2$ receptor channels (Ding and Sacks, 1999). In nominally Ca^{2+}-free solution the outside-out patches were unstable and the cell-attached patches were very noisy in the presence of IVM; hence, 1 mM $CaCl_2$ was used. The pipette solution contained (mM): 140 NaF, 5 NaCl, 10 EGTA, and 10 HEPES, adjust to pH 7.0 with NaOH, 315–320 mOsmol Kg^{-1}. F^- was used as the major anion in the pipette solution since it was very difficult to obtain an outside-out patch when only $Cl^-$was used. In whole-cell

experiments, the effects of IVM were the same when either Cl^- or F^- were the major intracellular anion. Single-channel currents were low-pass filtered at 5 kHz, digitized at 50 kHz, and stored on both VCR and computer. Occasional large brief noise spikes were visually identified and removed from the current traces. For the on-cell recordings, the pipette solution (external solution) contained (mM): 154 NaCl, 1 $CaCl_2$, and 10 HEPES, adjust to pH 7.4 with NaOH, 320–325 mOsmol Kg^{-1}. The currents were filtered and digitized as described for the outside-out patch configuration.

Data Analysis

The durations of open and shut intervals were measured with half-amplitude threshold analysis, as described previously (McManus and Magleby, 1988, 1991). The methods used to log bin the intervals into 1-D dwell-time distributions, fit the distributions with sums of exponentials using maximum likelihood fitting techniques (intervals less than two dead times were excluded from the fitting), and determine the number of significant exponential components with the likelihood ratio test, have been described previously (Blatz and Magleby, 1986; McManus and Magleby, 1988, 1991). The 1-D dwell-time distributions are plotted with the Sigworth and Sine (1987) transformation, as the square root of the number of intervals per bin with a constant bin width on logarithmic time axis.

To estimate the association rate constant, dissociation rate constant, and the equilibrium dissociation constant for the effects of IVM, it was assumed that there is no cooperativity in the binding of IVM, that the receptors are homogenous, and that the effects of IVM can be described by a second order reaction of the type:

$$R + M \underset{k_{-1}}{\overset{k_{+1}}{\rightleftharpoons}} RM$$

where R is the receptor (channel), M is the modulator (IVM), and K_{+1} and K_{-1} are the association and dissociation rate constants, respectively. Accordingly, the equilibrium dissociation constant (K_d) is given by:

$$K_d = \frac{k_{-1}}{k_1}.$$

The relationship between the association and dissociation rate constants and the time course of the observed changes in the current after the addition of IVM (τ_{on}) and after the washout of IVM (τ_{off}) are given by:

$$\frac{1}{\tau_{on}} = k_1 \times [M] + k_{-1}$$

$$\frac{1}{\tau_{off}} = k_{-1}.$$

RESULTS

Fig. 1 B shows membrane currents recorded in the whole-cell configuration of the patch-clamp technique in response to 10 μM extracellular ATP at a holding potential of −50 mV. The cell was continuously perfused with the standard extracellular solution while ATP was applied for 3 s every 3 min (indicated by short bars above the downward current traces). As a result of either partial recovery from desensitization or of rundown, the response to the second application of ATP in the control period was smaller than the first. However, after the addition of 3 μM IVM to the extracellular solution, the current in response to ATP increased while the current in the absence of ATP (holding current) was unchanged. After the removal of the IVM the ATP-induced currents returned to the control level. These effects of IVM are consistent with previous work on the rat $P2X_4$ receptor channel studied in *Xenopus* oocytes (Khakh et al., 1999; unpublished data).

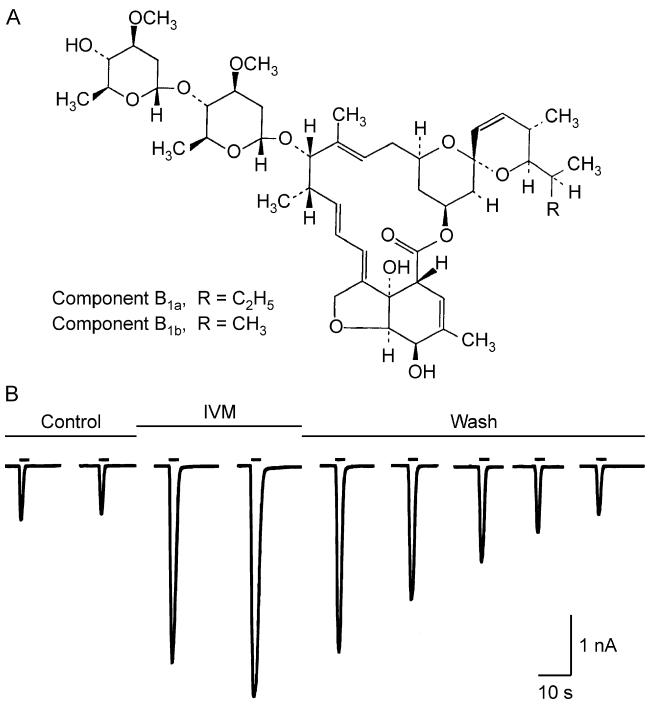

FIGURE 1. IVM reversibly augments the response of $hP2X_4$ to ATP. (A) The structure of IVM (taken from Merck Index). (B) Whole-cell current traces in response to ATP (10 μM) applied for 3 s every 3 min (short bars) before, during, and after the application of IVM (3 μM), as indicated above the current traces. Holding potential −50 mV.

IVM Does Not Modulate $hP2X_4$ Channels from within the Cell

The gradual onset and washout of the effects of IVM, as well as its lipophilic nature, suggest that IVM might need to penetrate the cell in order to modulate the channel. If this is the case, then IVM should be effective if directly introduced into the cell via the patch pipette. In such experiments, the first response to 10 μM ATP was measured 20 s after establishing the whole-cell configuration and thereafter at 3-min intervals. The response to the first application of ATP was taken to represent the control response to ATP. Intracellular IVM (3 μM) had no detectable effect on the amplitude or on the rate of deactivation of the current activated by ATP within 6 min. In contrast, 5 min after the addition of 3 μM IVM to the extracellular solution, the maximal current increased in the same cell 6.7-fold. A similar lack of effect of intracellular IVM and a significant ef-

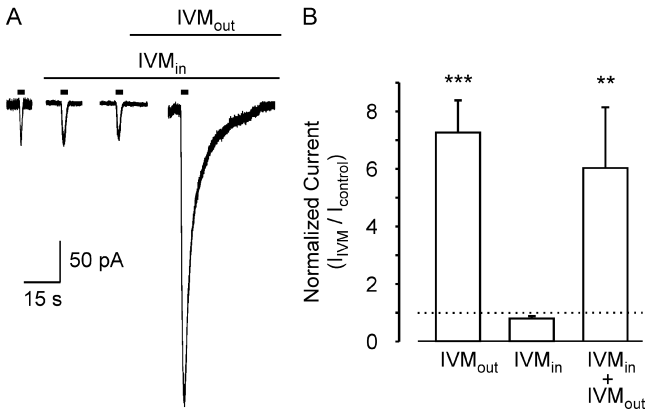

FIGURE 2. IVM does not modulate hP2X$_4$ receptor channels from within the cell. (A) Whole-cell current traces in response to ATP (3 μM) applied for 3 s every 3 min (short bars) before and after the addition of IVM (3 μM) to the extracellular solution, as indicated above the current traces. The first application of ATP was 20 s after establishing the whole-cell configuration. The standard pipette solution also contained IVM (3 μM). Holding potential of −50 mV. (B) Average (±SEM) amplitude of the whole-cell current activated by extracellular ATP (3 μM) 6 min after the addition of 3 μM IVM to the extracellular solution (IVM$_{out}$), 6 min after exposure to intracellular 3 μM IVM (IVM$_{in}$), or 5 min after the addition of 3 μM extracellular IVM to the cells exposed to intracellular IVM for 6 min (IVM$_{in}$ + IVM$_{out}$). The amplitudes were normalized to the control response (dashed line). The bars represent between 5–14 cells. The statistical significance between IVM$_{out}$ and IVM$_{in}$ was determinate with the unpaired Student's *t* test, where *** represent P < 0.001, and between IVM$_{in}$ + IVM$_{out}$ and IVM$_{in}$ with paired Student's *t* test, where ** represent P < 0.01.

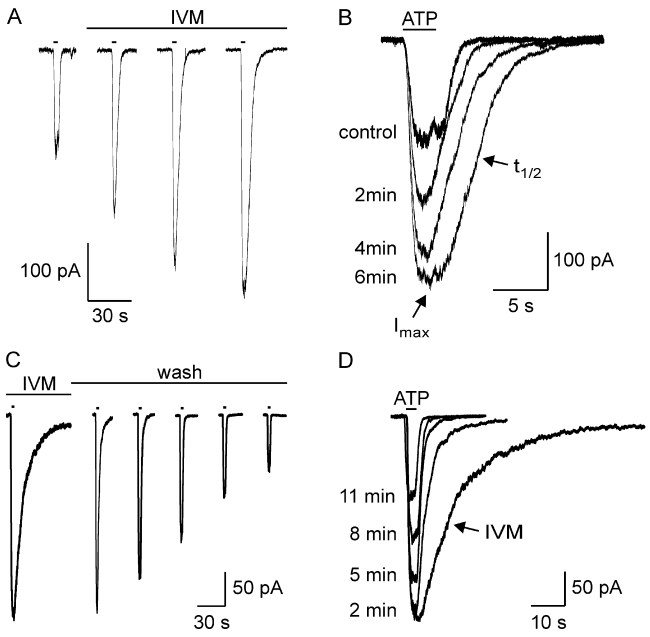

FIGURE 3. IVM has two distinct effects on hP2X$_4$ receptor channels. (A) Whole-cell current traces in response to ATP (3 μM) applied for 3 s every 2 min (short bars) before and during the application of IVM (3 μM), as indicated above the current traces. Holding potential of −60 mV. (B) Superposition of the current traces in A. (C) Whole-cell current traces in response to ATP (10 μM) applied for 3 s every 3 min (short bars) in the presence of IVM (3 μM) and after the washout IVM, as indicated above the current traces. The first exposure to ATP was after the cell was exposed to IVM (3 μM) for 6 min. IVM was washed out 50 s after the first application of ATP. Holding potential of −50 mV. (D) Superposition of the current traces in C.

fect of extracellular IVM was observed in five out of five experiments. On average, the enhancement in current amplitude induced by extracellular IVM in cells exposed to intracellular IVM was similar to the enhancement in current induced by extracellular IVM alone (Fig. 2 B). This indicates that intracellular IVM has no obvious effect on the hP2X$_4$ receptor channels. We conclude that IVM modulates the hP2X$_4$ receptor channels from outside the cell, though the possibility that IVM must partially embed in the membrane in order to modulate the channels cannot be excluded.

IVM has Two Distinct Effects on hP2X$_4$ Channels

To better resolve the onset of the effect of IVM, a lower concentration of ATP (3 μM) was applied. With this lower concentration of ATP the current largely recovered from desensitization within 2 min and thus the response to ATP could be probed at 2-min intervals. The current traces in response to ATP shown in Fig. 3 A are superimposed in Fig. 3 B. Similar to the effects of IVM on the P2X$_4$ receptor channel from rat (Khakh et al., 1999), IVM appeared to have at least two effects on the ATP-activated current: IVM increased the maximal current and slowed the rate of current deactivation after the washout of ATP. The distinct effects of IVM on current amplitude and on the rate of deactivation were more clearly resolved after the washout of IVM, as demonstrated in Fig. 3, C and D. The first current trace in Fig. 3 C shows the response to 10 μM ATP applied for 3 s to a cell exposed to 3 μM IVM for 6 min. ATP was then applied at 3-min intervals with the next application occurring 130 s after washing out the IVM. Within the 2 min of the washout of IVM, the pronounced effect of IVM on the rate of deactivation was greatly reduced, whereas the increase in current amplitude induced by IVM was almost unchanged. This differential rate of recovery from the effects of IVM, most clearly seen when the ATP-activated currents are superimposed (Fig. 3 D), unambiguously demonstrates that IVM exhibits two distinct actions on P2X receptor channels.

Fig. 4 summarizes the time course of the effects of IVM on current amplitude and on the rate of current deactivation. Fig. 4 A shows the time course of the average normalized change in the amplitude of the ATP-activated current (I$_{max}$) after the wash-in of 3 μM IVM

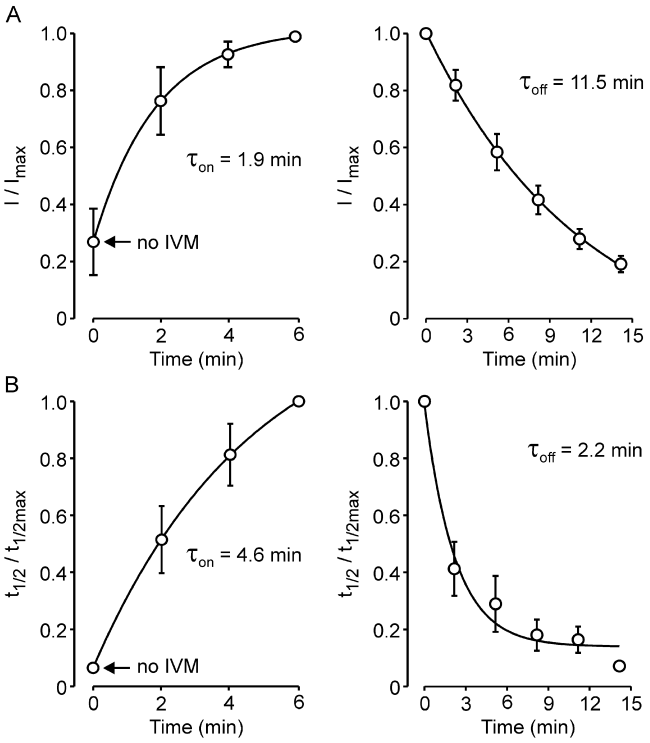

FIGURE 4. The changes in I_{max} and $t_{1/2}$ induced by IVM have distinct kinetics. Average (± SEM) normalized amplitude (A) and $t_{1/2}$ (B) of the whole-cell currents activated by extracellular ATP (3 μM) as a function of time after the addition of 3 μM IVM (left) and after the washout of IVM (right). The left and right graphs are the average of three and seven cells, respectively. The solid lines are exponential fits to the data.

(left) and after washout (right). Fitting single exponential functions to the data yielded time constants of 1.9 and 11.5 min, respectively (solid lines). As a first approximation, the apparent association rate constant, dissociation rate constant, and the equilibrium dissociation constant for the effect of IVM on current amplitude were estimated assuming a second order reaction to be 1.5×10^5 M^{-1} min^{-1}, 0.087 min^{-1}, and 5.9×10^{-7} M, respectively (see MATERIALS AND METHODS for details).

The time at which the current declined to half the maximal value ($t_{1/2}$) after the washout of ATP was taken as a measure of the rate of deactivation since the time course of current deactivation could not be fit by a single exponential. Fig. 4 B shows the average normalized change in $t_{1/2}$ induced by 3 μM IVM after wash-in (left) and after the washout of IVM (right). As for I_{max}, single exponential functions fit the data, with time constants of 4.6 and 2.2 min, respectively. However, the rate of recovery during washout was faster than the rate of onset, indicating that the effect of IVM on current deactivation is not a simple second order reaction. In other words, more than one IVM molecule likely binds to the receptor in order to induce a change in the rate of current deactivation (see DISCUSSION). The apparent deviation from second order reaction for the effects of IVM on $t_{1/2}$ as well as the difference in the rates of onset and recovery of the effect of IVM on I_{max} and on $t_{1/2}$ point to at least two distinct effects of IVM on the $hP2X_4$ receptor channel.

The Effects of IVM on Current Amplitude and on the Rate of Deactivation Have Distinct Concentration-response Relationships

IVM is a mixture of >90% of 22,23-dihydroavermectin B_{1a} and <10% of 22,23-dihydroavermectin B_{1b} (Fig. 1 A). Hence, is it possible that the two components of IVM bind to the same site with different affinities and have disparate effects on channel gating? In this case, the concentration dependence for the two effects should be identical because the ratio of the two components does not change as the concentration of the mixture is changed. At equilibrium, the ratio of channels bound by the B_{1a} and B_{1b} components will remain fixed as long as the ratio of the two components in the solution is constant. To examine this possibility we studied the concentration dependence for the two effects of IVM on the $P2X_4$ receptor channel. Each cell was exposed to ATP (3 μM) for 3 s under control conditions and after exposing the cell to IVM for 5 min, and I_{max} of the second application of ATP was then normalized to I_{max} of the first application of ATP. An incubation time of 5 min in IVM was chosen in order to minimize the effects of desensitization/rundown, and since the effect of IVM on I_{max} approached steady-state by this time (Fig. 4 A). The concentration-response relationship for the effect of IVM on I_{max} is presented in Fig. 5 (circles). The concentration-response relationship was fitted by the Hill equation:

$$y = y_{con} + \frac{a[IVM]^n}{[IVM]^n + EC_{50}{}^n},$$

where y is I_{max} in response to 3 μM ATP at a given concentration of IVM, y_{con} is I_{max} in response to 3 μM ATP in the absence of IVM, a is the maximal fold increase in I_{max} induced by IVM, n is the Hill coefficient, and EC_{50} is the concentration of IVM ([IVM]) yielding an effect half the maximum. From the fit, EC_{50} was estimated to be 0.25 ± 0.02 μM, similar to the equilibrium dissociation constant calculated from the association and dissociation rate constants (0.59 μM). The Hill coefficient (n) and the maximal increase in current amplitude (a) were estimated to be 2.4 ± 0.5- and 6.6 ± 0.3-fold, respectively.

The equilibrium dissociation constant for the effect of IVM on $t_{1/2}$ was initially approximated by constructing an IVM concentration-response relationship from the currents measured after 5 min in IVM (Fig. 5, filled

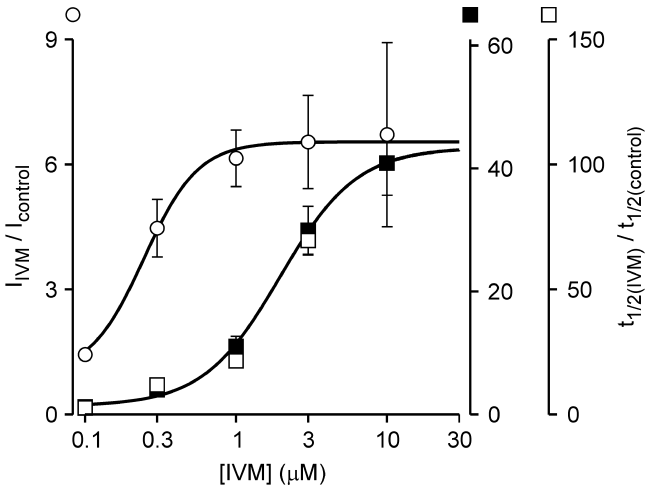

FIGURE 5. The two effects of IVM have distinct affinities to IVM. Normalized concentration-response relationships for the effects of IVM on I_{max} (empty circles) and on $t_{1/2}$ (full squares). Each point represents the average (±SEM) response of six cells 5 min after the addition of IVM. Solid lines are fits to the Hill equation with EC_{50} and n of 0.25 μM and 2.4, and 2.0 μM and 1.7 for I_{max} and $t_{1/2}$, respectively. The concentration-response relationship for $t_{1/2}$ 20 min after the addition of IVM is also shown (empty squares).

squares). The Hill equation was fitted to the concentration-response relationship giving an EC_{50}, n, and a of 2.0 ± 0.1, 1.7 ± 0.2, and 42 ± 2-fold μM, respectively. After 5-min incubation with 3 μM IVM, the effect of IVM on $t_{1/2}$ is ~75% of the maximal effect (Fig. 4 B). To test to what extent the data at 5 min reflects the steady-state concentration-response relationship, the effect of IVM on $t_{1/2}$ after 20 min was examined. The normalized concentration-response relationships for 5- and 20-min incubation in IVM are similar (Fig. 5), indicating that the initial estimate of EC_{50} and n represent the steady-state effects of IVM on $t_{1/2}$. Thus, the concentration-response relationships for the effects of IVM on I_{max} and on $t_{1/2}$ are indeed displaced in relation to each other.

These results indicate that the two effects of IVM cannot be attributed to distinct effects of the B_{1a} and B_{1b} components binding to the same site. We conclude, therefore, that IVM binds to two separate sites on the $hP2X_4$ receptor channel: a higher affinity site that primarily affects I_{max} and a lower affinity site which affects $t_{1/2}$ (see DISCUSSION).

IVM Modulates the Efficacy of ATP

To determine whether IVM has an effect on the efficacy of ATP, concentration-response relationships for the effect of ATP were constructed in the absence and presence of IVM. To this end, whole-cell currents were recorded using the perforated-patch whole-cell configuration of the patch-clamp technique to avoid the decline in current amplitude observed in the conventional whole-cell configuration during repeated ATP applications. A concentration-response relationship for the effect of ATP in the absence of IVM was constructed first. For each cell, different concentrations of ATP were applied, and each tested concentration of ATP was bracketed by a measurement with 3 μM ATP. The currents were then normalized to the current activated by the preceding dose of 3 μM ATP. Only cells in which the response to 3 μM ATP did not change by >20% were analyzed further. Fig. 6 A shows superimposed current traces measured from a single cell in response to 0.3, 1, 3, or 100 μM ATP applied for 2 s under control conditions. The resulting concentration-response relationship for ATP in the absence of IVM (averaged from seven experiments) is shown in Fig. 6 B (empty circles). The Hill equation was fitted to the data (solid line) with an EC_{50} n and maximal current of 3.8 ± 0.8 μM, 0.8 ± 0.1, and 300 ± 16 pA, respectively.

Next, cells were exposed either to 0.2 μM IVM, a concentration of IVM which primarily affects I_{max} (Fig. 5) or to 1.0 μM IVM, which also affects $t_{1/2}$ (Fig. 5). Each cell was exposed to IVM for at least 25 min before current recording was attempted in order to provide sufficient time for IVM to equilibrate (see Fig. 4). The resulting concentration-response relationships for added ATP, averaged from eight experiments for 0.2 μM IVM (filled circles) and seven experiments for 1.0 μM IVM (filled inverted triangles), are shown in Fig. 6 B. The EC_{50}, n, and maximal current obtained from fitting the concentration-response relationships with the Hill equation (solid lines in Fig. 6 B) are: 2.5 ± 0.7 μM, 1.2 ± 0.3, and 1,200 ± 110 pA, and 0.5 ± 0.1 μM, 2.7 ± 0.6, and 1,100 ± 50 pA, for 0.2 μM IVM and 1.0 μM IVM, respectively. It appears from these results that the higher affinity site for IVM primarily increased the maximal response to ATP while the lower affinity site for IVM primarily increased the sensitivity to ATP and the apparent cooperativity of ATP.

The Effects of IVM on Unitary $hP2X_4$ Receptor Channel Currents Measured in the Outside-out Configuration of the Patch-clamp Technique

Together, the results presented thus far are consistent with two distinct allosteric effects of IVM on the $hP2X_4$ receptor channel. To resolve the mechanisms by which IVM increases the maximal current and slows the rate of deactivation, single channel currents were measured. Single-channel currents activated by extracellular ATP were initially recorded in the outside-out configuration of the patch-clamp technique. The membrane potential was held at −150 mV since the conductance of $P2X_4$ receptor channels is relatively small (Evans, 1996; Negulyaev and Markwardt, 2000). The pipette contained the standard intracellular solution and the patch of membrane was continuously perfused with the standard extracellular solution. Upon exposing the patch to extra-

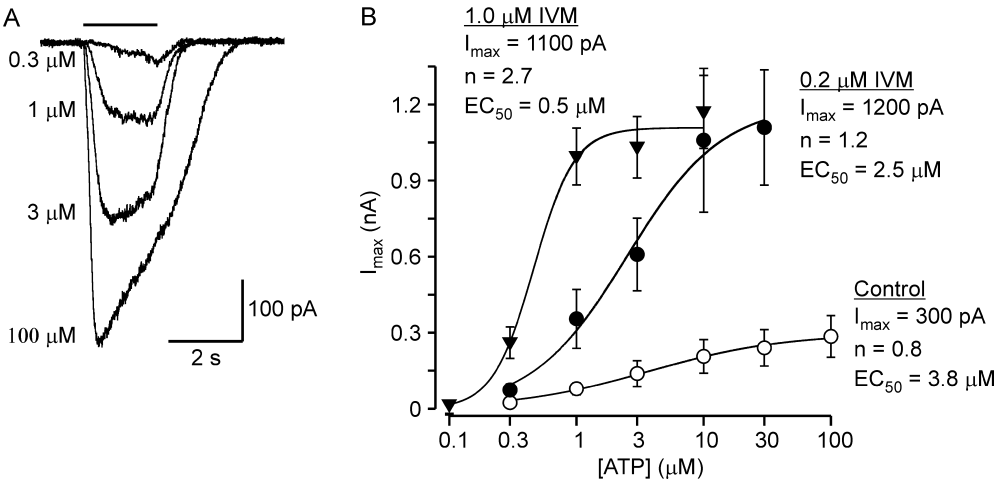

FIGURE 6. The functionally distinct sites for IVM have different effects on the efficacy of ATP. (A) Perforated-patch whole-cell current traces in response to different concentrations of ATP applied for 2 s, as indicated. Holding potential −50 mV. (B) Concentration-response relationships for ATP in the absence (empty circles) or presence of either 0.2 μM (full circles) or 1.0 μM (full inverted triangles) IVM. Each point represents the average (±SEM) of 6–8 cells. Solid lines are fits to the Hill equation.

cellular ATP (0.3–100 μM) bursts of channel activity were detected in 76 of 264 outside out patches tested. However, in all but 3 of the 76 patches channel activity was lost within 40 s and did not recover following several minutes of wash in the absence of ATP. One of the three patches in which channel activity persisted for several minutes is presented in Fig. 7. Representative current traces recorded in the presence of 3 μM ATP are shown. Downward (inward) current deflections indicate channel opening and the dashed lines indicate the average current level in the main conducting state in the absence of IVM (control). Initially, ATP was applied for 5 s under control conditions (top current trace). Subsequently, the patch was exposed to 3 μM IVM for 6 min and ATP applied again for 5 s (IVM_1). In the presence of IVM the baseline current tended to fluctuate, and the current recordings were typically noisier than in the absence of IVM. Nevertheless, it is clearly evident that in the presence of IVM channel open time is greatly increased. A small (~20%) increase in the unitary current amplitude with IVM is also apparent. When IVM was washed out for 6 min and ATP was applied again ($wash_1$), the effect of IVM on channel open time was greatly reduced. The application and washout of IVM were repeated at 6-min intervals (IVM_2 and $wash_2$), revealing once again the significant effect of IVM on the open time of the channel. These results clearly indicate that the sixfold increase in I_{max} in saturating ATP concentrations observed in whole-cell recordings in response to IVM (Fig. 6 B) is primarily not due to an increase in unitary conductance and likely involves changes in channel gating.

The Effects of IVM on Unitary hP2X$_4$ Receptor Channel Currents Determined from On-cell Patches

The rapid loss of channel activity in excised patches of membrane suggests that an intracellular factor is important for continued channel function. To obtain sufficient single-channel data to quantify the effects of IVM on channel gating, channel activity was recorded in the cell-attached mode of the patch-clamp technique. The cells were bathed in a solution containing 150 mM KCl in order to shunt the membrane potential to zero, whereas the patch of membrane underlying the pipette was clamped to −150 mV. Although it is possible to change the composition of the solution in the pipette during on-cell recording, this is a rather slow process and it is difficult to determine when complete solution exchange has taken place. We, therefore, measured channel activity under a single experimental condition in each patch, and made comparisons between patches exposed to ATP alone (control) and patches exposed to ATP plus 0.3 or 1.5 μM IVM. These concentrations of IVM were chosen since 0.3 μM IVM primarily modified I_{max} in the whole-cell recordings while 1.5 μM IVM modified both I_{max} and $t_{1/2}$ (Fig. 5). To provide sufficient time for IVM to equilibrate (see Fig. 4), the cells were preincubated with IVM for 20–25 min before forming a tight seal and the recording pipette also contained the appropriate concentration of IVM. A relatively low concentration of ATP (0.3 μM) was used in the pipette solution in order to minimize the simultaneous activation of multiple channels and to limit channel desensitization.

Without ATP in the pipette solution, there were no channel openings resembling hP2X$_4$ receptor channel currents in either the absence (n = 30) or presence (n = 20) of IVM. In contrast, with 0.3 μM ATP in the pipette, a channel with a unitary conductance of ~12 pS at −150 mV was observed in 96 of 197 patches. In these patches, channel activity disappeared after several minutes, suggesting that even at low ATP concentrations the channels enter a long-lasting desensitized state. Fig. 8 A shows representative current records in the absence and presence of either 0.3 or 1.5 μM IVM, as indicated above each current trace. The downward deflections in the current indicate channel openings

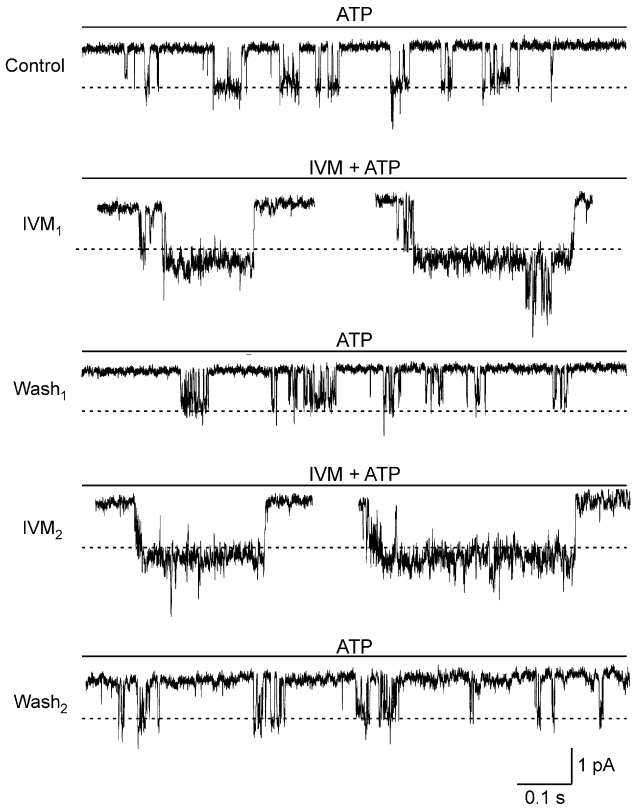

FIGURE 7. Representative current records from an excised outside-out membrane patch exposed to 3 μM ATP. Downward (inward) currents indicate channel opening. Shown is channel activity under control conditions (control), 6 min after exposing the patch to 3 μM IVM (IVM_1) and 6 min after washing out the IVM ($wash_1$). The application and washout of IVM were repeated (IVM_2 and $wash_2$). The dashed lines present the average current of the main conductance state during the first exposure to ATP (control). Holding potential −150 mV. Sampled at 50 kHz and filtered at 1 kHz for display.

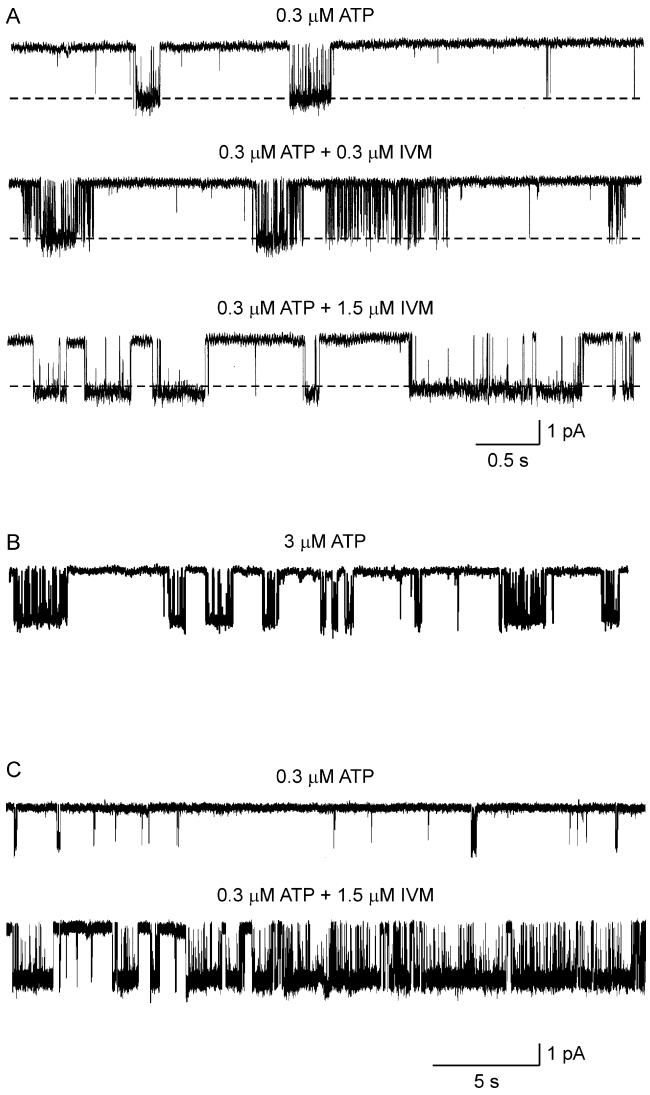

FIGURE 8. The effects of IVM on unitary $hP2X_4$ receptor channel currents in on-cell patches. (A) Representative current records from three different on-cell patches. The pipette solution contained extracellular solution supplemented with 0.3 μM ATP (top trace), 0.3 μM ATP plus 0.3 μM IVM (middle trace), or 0.3 μM ATP plus 1.5 μM IVM (bottom trace). When IVM was included in the pipette solution, the cell was incubated in the same concentration of IVM for at least 25 min before establishing the cell-attached configuration. The dashed lines present the average current in the open state under control conditions. Sampled at 50 kHz and filtered at 1 kHz for display. (B) Representative single-channel current record with 3 μM ATP in the pipette solution. Same calibration as in A. Note the brief openings within the burst in comparison to the long openings induced by 1.5 μM IVM. (C) Representative current records 30 s in duration, from two different on-cell patches. The pipette solution contained extracellular solution supplemented with 0.3 μM ATP (top trace) or 0.3 μM ATP plus 1.5 μM IVM (bottom trace). Same experimental protocol as in A.

and the dashed lines represent the average current level in the open state measured in the absence of IVM. It is immediately apparent that as in the outside-out patches, IVM had a small (but statistically significant) effect on the unitary current amplitude. On average, the conductance of the channel in the absence of IVM was 11.8 ± 0.8 pS ($n = 5$), increasing to 15.3 ± 0.7 pS in 1.5 μM IVM ($n = 5$), ($P < 0.05$, unpaired Student's t test). It is also clearly evident that 1.5 μM IVM considerably prolonged the open times. This increase in open time is not due to the greater potency of ATP in the presence of IVM (Fig. 6 B), since raising the concentrations of ATP in the absence of IVM did not significantly prolong the mean open time (Fig. 8 B). Fig. 8 C shows examples of 30 s of continuous current recordings under control conditions (top trace) and in the presence of 1.5 μM IVM. The absence of superimposed channel openings despite the significant channel activity in the patch exposed to 1.5 μM IVM indicates that IVM significantly increases Po (see also Table I). Whether IVM also recruits silent channels remains to be determined.

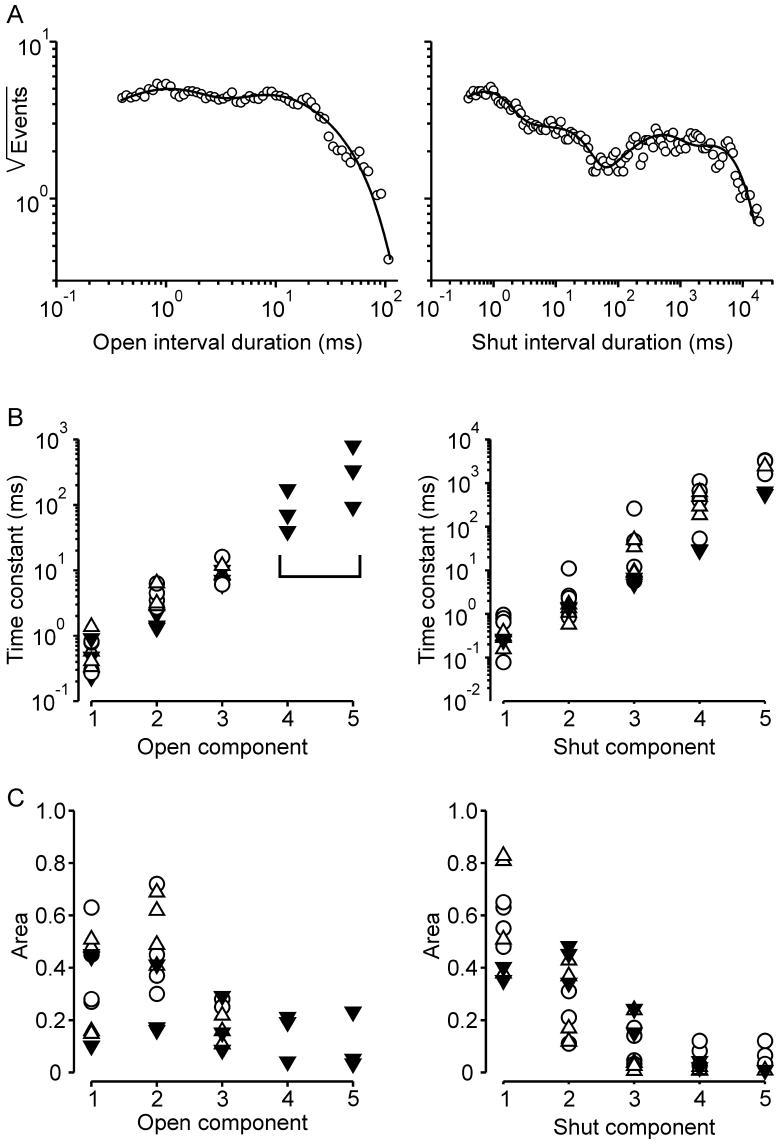

FIGURE 9. The effects of IVM on hP2X$_4$ receptor channel gating are complex. (A) Distributions of open (left) and shut (right) interval durations for unitary hP2X$_4$ receptor channel activity recorded from an on-cell patch in response to 0.3 μM ATP under control conditions. The solid lines are the maximum likelihood fits with sums of exponentials. The open and shut intervals were described by the sum of three and five significant exponential components, respectively (patch c02 in Table I). (B and C) Time constants (B) and areas (C) of the open (left) and shut (right) significant exponential components fitted to the dwell-time distributions of the channels exposed to 0.3 μM ATP alone (open circles), 0.3 μM ATP plus 0.3 μM IVM (empty triangle), or 0.3 μM ATP plus 1.5 μM IVM (full triangle). The values are presented in Table I.

Gating Properties of the hP2X$_4$ Receptor Channel

In the control experiments and in most of the experiments with 0.3 μM IVM it was not possible to determine the total number of channels in the patch or whether two adjacent bursts of channel openings were from the same or different channels due to the relatively low Po. Consequently, kinetic analysis was largely restricted to the number and duration of open and shut events within a burst of channel activity and to the duration of the bursts using patches for which at least 1,200 open and shut events could be analyzed. The durations of all open and shut intervals were measured first with half-amplitude threshold analysis. The open and shut intervals were then log-binned into 1-D dwell-time distributions and the distributions were fit with sums of exponentials to determine the number of significant exponential components. Fig. 9 A plots open and shut dwell-time distributions for one experiment recorded under control conditions. The open (left panel) and shut (right panel) distributions were best fit with the sums of three and five significant exponential components, respectively (continuous lines). The time constants and magnitudes of the significant exponential components fit to the open and shut dwell time distributions for the control patches (open circles), the patches in 0.3 μM IVM (open triangles), and the patches in 1.5 μM IVM (filled inverted triangles) are summarized in Fig. 9, B and C, and in Table I. As might be expected from the single-channel current traces (Figs. 7 and 8), it is evident that 1.5 μM IVM gave rise to two open states of long duration not observed under control conditions or in the presence of 0.3 μM IVM. It is also apparent from Fig. 9 B that the three longest shut components were reduced in duration by 1.5 μM IVM, consistent with the increase in Po induced by IVM (Fig. 8 C). The

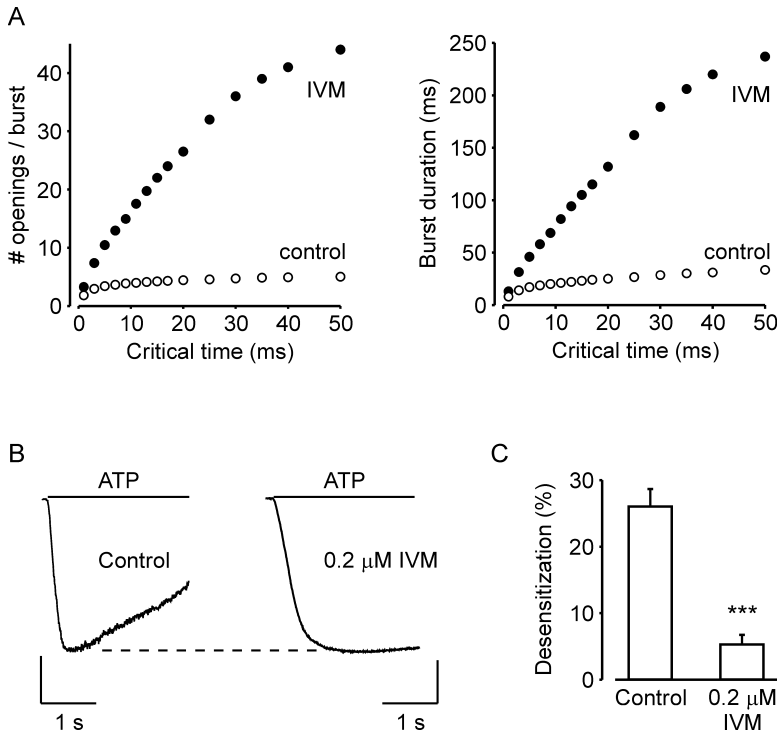

FIGURE 10. The higher affinity site of IVM reduces $hP2X_4$ receptor channel desensitization. (A) Number of opening per burst (left) and burst duration (right) induced by 0.3 μM ATP as a function of the critical time between bursts of channel activity in the absence (open circles) or presence of 0.3 μM IVM (full circles). (B) Perforated-patch whole-cell currents in response to 2-s application of 30 μM ATP in the absence (left) and presence (right) of 0.2 μM IVM. The cell was incubated for 30 min with 0.2 μM IVM before exposure to ATP. Holding potential −60 mV. Calibration bars, 150 pA (left) and 500 pA (right). (C) Average (±SEM) desensitization after 2-s exposure to 30 μM ATP in the absence (control) and presence of 0.2 μM IVM ($n = 8$). The statistical significance between the groups was determinate with unpaired Student's t test, where *** represent $P < 0.001$.

time constants of the two most brief shut components were not significantly affected by 1.5 μM IVM despite the overall increase in Po, suggesting that these components represent shut events within a burst of channel activity.

In 1.5 μM IVM it was not possible to reliably determine a minimal shut time (critical time) that would define the end of a burst since the third shut component (counting from the most brief component) was only 3–5-fold longer than the second component. Hence, burst analysis was used only to compare between the control experiments and the experiments in 0.3 μM IVM. To prevent possible errors arising from the selection of a specific critical time, critical times ranging from 1 to 50 ms were examined. Fig. 10 A shows the number of openings per burst (left) and burst duration (right) as a function of critical time under control conditions (open circles) and in the presence of 0.3 μM IVM (filled circles). Although the bursts are not well separated for this channel, it is evident that 0.3 μM IVM increased both the number of openings per burst and burst duration for all tested critical times. An increase in burst duration that is not accompanied by an increase in mean open time or mean shut time within a burst could arise from a greater efficacy of ATP, and/or from reduced channel desensitization. However, since low concentrations of IVM had little effect on the EC_{50} of the ATP concentration-response relationship (Fig. 6 B), the increase in burst duration is likely due to reduced channel desensitization. This conclusion is supported by measurements of the effects of 0.2 μM IVM on the rate of deactivation of whole-cell currents activated by 30 μM ATP (Fig. 10, B and C).

In summary, 0.3 μM IVM increased burst duration without significantly affecting mean open time or single-channel conductance, whereas 1.5 μM IVM substantially prolonged mean open time and increased the probability of channel opening. The relationship of these effects of IVM to the changes in ensemble ATP-activated currents is addressed in the DISCUSSION.

DISCUSSION

The aim of this study was to examine the mechanism underlying the actions of IVM on the human $P2X_4$ receptor channel. From the whole-cell data it is clear that IVM at concentrations >1 μM has two distinct effects on $hP2X_4$ receptor channels: up to a sixfold increase in the maximum current activated by saturating concentrations of ATP, and up to a 10-fold slowing of the rate of current deactivation (Fig. 5). These two phenomena can be explained by assuming that IVM binds to separate sites, with the increase in maximal current resulting from the binding of IVM to a higher affinity site than the site that leads to a reduction in the rate of deactivation. This assertion is based on the following observations: (a) The time courses of onset and washout of the effect of IVM on I_{max} and on $t_{1/2}$ were significantly different (Fig. 4). (b) The effect of IVM on $t_{1/2}$ deviates from a second order reaction (Fig. 4). (c) The effects of IVM on I_{max} and on $t_{1/2}$ have distinct concentration-response relationships (Fig. 5). (d) Low concen-

TABLE I

Significant Exponential Components Fit to the Open and Shut Dwell Time Distributions

Patch	IVM	Events	Po	Mean open	Open components Time constant and (area)					Shut components Time constant and (area)				
					1	2	3	4	5	1	2	3	4	5
	μM		%	*ms*	*ms*	*ms*	*ms*	*ms*	*ms*	*ms*	*ms*	*ms*	*ms*	*ms*
C02		2,018	2	3.4	0.30 (0.27)	2.7 (0.45)	6.1 (0.28)			0.95 (0.63)	11 (0.11)	260 (0.14)	1,100 (0.12)	
C04		1,382	0.7	1.9	0.79 (0.63)	3.5 (0.37)				0.078 (0.55)	0.85 (0.31)	5.7 (0.046)	53 (0.026)	1,600 (0.065)
C05		1,992	2	3.9	0.27 (0.28)	4.5 (0.72)				0.79 (0.65)	2.6 (0.21)	47 (0.032)	660 (0.082)	3,300 (0.032)
C07		2,182	1.5	6.8	0.82 (0.45)	6.3 (0.30)	16 (0.25)			0.65 (0.48)	2.3 (0.11)	12 (0.17)	400 (0.12)	3,200 (0.12)
I031	0.3	1,862	7.8	4	0.34 (0.16)	2.9 (0.62)	8.5 (0.22)			0.16 (0.51)	0.59 (0.43)	9.5 (0.039)	190 (0.011)	2,500 (0.009)
I034	0.3	5,218	43	3.8	0.42 (0.15)	3.2 (0.69)	8.8 (0.16)			0.32 (0.81)	1.1 (0.17)	35 (0.008)	300 (0.009)	
I038	0.3	4,152	20	3.2	0.59 (0.48)	3.2 (0.41)	12 (0.11)			0.29 (0.38)	1.7 (0.37)	8.9 (0.24)	640 (0.012)	
I039	0.3	2,622	18	4	1.4 (0.51)	6.5 (0.49)				0.39 (0.83)	1.4 (0.12)	51 (0.027)	500 (0.023)	
I151	1.5	18,046	80	35	0.23 (0.10)	2.1 (0.17)	10 (0.29)	39 (0.21)	92 (0.23)	0.26 (0.35)	1.3 (0.48)	6.5 (0.15)	28 (0.041)	620 (0.007)
I152	1.5	3,390	96	66	0.90 (0.45)	1.3 (0.16)	6.0 (0.15)	170 (0.19)	790 (0.050)	0.26 (0.35)	1.3 (0.45)	6.5 (0.15)	28 (0.041)	620 (0.007)
I159	1.5	23,100	73	16	0.47 (0.44)	1.4 (0.41)	7.0 (0.084)	69 (0.040)	330 (0.032)	0.24 (0.40)	1.4 (0.34)	4.7 (0.24)	29 (0.017)	540 (0.006)

trations of IVM primarily increase the maximal response to ATP, whereas higher concentrations of IVM primarily increase the apparent affinity for ATP (Fig. 6 B). (e) The single-channel behavior of $hP2X_4$ receptor channels are distinct at low and high concentrations of IVM (Figs. 8 and 9).

There is insufficient data to construct a kinetic scheme which incorporates the effects of IVM on the gating of $hP2X_4$ receptor channels. Nevertheless, since functional P2X receptor channels likely contain three subunits (Nicke et al., 1998; Stoop et al., 1999), it is tempting to speculate that each channel has three identical binding sites for IVM. In this case, perhaps the binding of one molecule of IVM is sufficient to induce the observed effects of IVM on I_{max}. In contrast, the binding of a single molecule of IVM cannot account for the effects of IVM on $t_{1/2}$, since a single binding site cannot give rise to a rate of recovery during washout that is faster than the rate of onset (Fig. 4 B). Hence, we speculate that through allosteric interaction, the binding of the first molecule of IVM reduces the affinity of additional IVM molecules binding to the receptor (negative cooperativity). However, when one or two additional molecules of IVM bind to the receptor, the open state of the channel is greatly stabilized, giving rise to a substantial slowing of the rate of current deactivation. This model accounts for the higher concentrations of IVM needed to induce changes in $t_{1/2}$ in comparison to I_{max} and can account for the apparent deviation from second order reaction for the effects of IVM on $t_{1/2}$.

The slow onset and washout of the effects of IVM suggests that IVM, which is lipophilic, might need to partition into the membrane to reach its binding sites. If this is the case, these sites must be close to the extracellular face of the membrane since intracellular IVM had no apparent effect on channel gating (Fig. 2). The binding site for IVM appears to be extracellular in other channels as well, including the crayfish multiagonist–gated chloride-selective channel where application of IVM to the cytoplasmic side of inside-out patches had no effect (Zufall et al., 1989), and the glutamate-gated chloride channel from *Drosophila melanogater* (Cully et al., 1996) and the α7 nicotinic receptor (Krause et al., 1998) that could be activated by extracellular $IVMPO_4$, a hydrophilic form of IVM.

In an attempt to identify the molecular mechanisms underlying the effects of IVM, we examined single-channel activity in the absence and presence of IVM. Under control conditions, 2–3 and 4–5 significant exponential components fit the distributions of open and shut durations, respectively (Fig. 9). These observations suggest that $hP2X_4$ receptor channels gate among a minimum of three open and five shut states. At low concentrations (0.3 μM), IVM had minor effects on the number, duration, or area of the open and shut components (Table I). In contrast, at a higher concentration (1.5 μM), IVM gave rise to two additional open components of long duration, reduced the duration of the three longest shut components, and reduced the area of the shortest and two longest shut components. These results indicate that the effects of IVM on channel gating are highly complex and, thus, it was not feasible to construct a kinetic model for the effects of IVM on channel gating. To achieve this goal it would be necessary to examine the effects of multiple concentrations of IVM on patches containing a single channel. This could not be achieved due to the rundown of channel activity in outside out patches.

There were no significant effects of low concentrations of IVM on mean open time, or on single-channel conductance, whereas burst duration increased 3–5-

fold (for critical times between 5 and 20 ms). The absence of an obvious change in either the mean open time or mean shut time per burst (Table I) or in the apparent affinity for ATP (Fig. 6 B), suggests that the increase in burst duration induced by low concentrations of IVM results from less desensitization. We propose that in the absence of IVM the channels enter a desensitized state after activation within tens of milliseconds from which they can recover at a relatively low rate (hundreds of milliseconds). As a result, when ATP is applied under control conditions a fraction of the channels desensitize before the current fully develops. If IVM diminishes desensitization (either by increasing the rate of recovery from desensitization or by slowing the rate of entry into the desensitized state), then the number of channels contributing to the maximal current would increase substantially, giving rise to an increase in I_{max}.

Burst analysis could not be reliably applied to channel activity in 1.5 μM IVM due to the high Po. Nevertheless, the striking effect of high concentrations of IVM on mean-channel open time can largely account for the significant decrease in the rate of current deactivation after the washout of ATP observed in whole-cell recordings. In view of the significant effects of IVM on the stability of the open conformation of the channel, it is tempting to speculate that the observed increase in the potency of ATP (Fig. 6 B) reflects effects of IVM on channel gating rather then on the binding site for ATP.

In humans, IVM is typically given as an oral dose of 150 mg/kg, once a year. This dose, which has minimal adverse effects, results in a peak plasma concentration of IVM of ~50 ng/ml. In a recent study, higher concentrations of IVM were tested, resulting in a threefold greater peak plasma concentration, also with no significant adverse experiences (Guzzo et al., 2002). In view of the broad distribution of $P2X_4$ receptor channel mRNA in human tissues (Garcia-Guzman et al., 1997) and given that the EC_{50} for the high affinity site for IVM was 0.25 μM, which is ~220 ng/ml, it is surprising that IVM is so well tolerated. The tolerability of IVM is likely due in part to its exclusion from the central nervous system by P-glycoproteins in the endothelial cells of brain capillary (Lankas et al., 1997; Nobmann et al., 2001). This could not explain, however, the limited adverse effects of IVM on peripheral tissues. $P2X_4$ receptor channel mRNA is abundant in human heart, adrenal, liver, kidney, skeletal muscle, and trachea (Garcia-Guzman et al., 1997), and in rat, $P2X_4$ receptor channel protein is extensively expressed in epithelia, vascular and visceral smooth muscle, and fat cells (Bo et al., 2003). These findings might indicate that native human peripheral $P2X_4$ receptor subunits are in association with other subunits, which reduce or eliminates the sensitivity of the receptor to IVM, or that native human $P2X_4$ receptor channels are less sensitive to IVM either due to regulatory mechanisms or due to inaccessibility of the binding sites to IVM.

We thank Florentina Soto and Walter Stühmer for providing HEK293 cells transfected with the human $P2X_4$ receptor channel, and Karl Magleby for single channel analysis programs. Thanks to Miguel Holmgren, Karl Magleby, Joe Mindell, and Kenton Swartz for helpful discussions.

This research was supported by a grant from G.I.F., the German-Israeli Foundation for Scientific Research and Development, and by the Zlotowski Center for Neuroscience.

Olaf S. Andersen served as editor.

Submitted: 1 December 2003
Accepted: 26 January 2004

REFERENCES

Adelsberger, H., A. Lepier, and J. Dudel. 2000. Activation of rat recombinant $\alpha_1,\beta_2,\gamma_{2S}$ $GABA_A$ receptor by the insecticide ivermectin. *Eur. J. Pharmacol.* 394:163–170.

Blatz, A.L., and K.L. Magleby. 1986. Correcting single channel data for missed events. *Biophys. J.* 49:967–980.

Bo, X., M. Kim, S.L. Nori, R. Schoepfer, G. Burnstock, and R.A. North. 2003. Tissue distribution of $P2X_4$ receptors studied with an ectodomain antibody. *Cell Tissue Res.* 313:159–165.

Bowler, J.W., R.J. Bailey, R.A. North, and A. Surprenant. 2003. $P2X_4$, $P2Y_1$ and $P2Y_2$ receptors on rat alveolar macrophages. *Br. J. Pharmacol.* 140:567–575.

Burkhart, C.N. 2000. Ivermectin: an assessment of its pharmacology, microbiology and safety. *Vet. Hum. Toxicol.* 42:30–35.

Cully, D.F., D.K. Vassilatis, K.K. Liu, P.S. Paress, L.H. Van der Ploeg, J.M. Schaeffer, and J.P. Arena. 1994. Cloning of an avermectin-sensitive glutamate-gated chloride channel from *Caenorhabditis elegans*. *Nature.* 371:707–711.

Cully, D.F., P.S. Paress, K.K. Liu, J.M. Schaeffer, and J.P. Arena. 1996. Identification of a *Drosophila melanogaster* glutamate-gated chloride channel sensitive to the antiparasitic agent avermectin. *J. Biol. Chem.* 271:20187–20191.

Dawson, G.R., K.A. Wafford, A. Smith, G.R. Marshall, P.J. Bayley, J.M. Schaeffer, P.T. Meinke, and R.M. McKernan. 2000. Anticonvulsant and adverse effects of avermectin analogs in mice are mediated through the γ-aminobutyric $acid_A$ receptor. *J. Pharmacol. Exp. Ther.* 295:1051–1060.

Dent, J.A., M.W. Davis, and L. Avery. 1997. avr-15 encodes a chloride channel subunit that mediates inhibitory glutamatergic neurotransmission and ivermectin sensitivity in *Caenorhabditis elegans*. *EMBO J.* 16:5867–5879.

Dent, J.A., M.M. Smith, D.K. Vassilatis, and L. Avery. 2000. The genetics of ivermectin resistance in *Caenorhabditis elegans*. *Proc. Natl. Acad. Sci. USA.* 97:2674–2679.

Ding, S., and F. Sacks. 1999. Ion permeation and block of $P2X_2$ purinoceptors: single channel recordings. *J. Membr. Biol.* 172:215–223.

Evans, R.J. 1996. Single channel properties of ATP-gated cation channels (P2X receptors) heterologously expressed in Chinese hamster ovary cells. *Neurosci. Lett.* 212:212–214.

Feng, X.P., J. Hayashi, R.N. Beech, and R.K. Prichard. 2002. Study of the nematode putative GABA type-A receptor subunits: evidence for modulation by ivermectin. *J. Neurochem.* 83:870–878.

Garcia-Guzman, M., F. Soto, J.M. Gomez-Hernandez, P.E. Lund, and W. Stühmer. 1997. Characterization of recombinant human P2X4 receptor reveals pharmacological differences to the rat ho-

mologue. *Mol. Pharmacol.* 51:109–118.

Guzzo, C.A., C.I. Furtek, A.G. Porras, C. Chen, R. Tipping, C.M. Clineschmidt, D.G. Sciberras, J.Y. Hsieh, and K.C. Lasseter. 2002. Safety, tolerability, and pharmacokinetics of escalating high doses of ivermectin in healthy adult subjects. *J. Clin. Pharmacol.* 42:1122–1133.

Hamill, O.P., A. Marty, E. Neher, B. Sakmann, and F.J. Sigworth. 1981. Improved patch-clamp techniques for high-resolution current recording from cells and cell-free membrane patches. *Pflugers Arch.* 391:85–100.

Horn, R., and A. Marty. 1988. Muscarinic activation of ionic currents measured by a new whole-cell recording method. *J. Gen. Physiol.* 92:145–159.

Khakh, B.S., W.R. Proctor, T.V. Dunwiddie, C. Labarca, and H.A. Lester. 1999. Allosteric control of gating and kinetics at $P2X_4$ receptor channels. *J. Neurosci.* 19:7289–7299.

Kim, Y.K., E.R. Dirksen, and M.J. Sanderson. 1993. Stretch-activated channels in airway epithelial cells. *Am. J. Physiol.* 265:C1306–C1318.

Köhler, P. 2001. The biochemical basis of anthelmintic action and resistance. *Int. J. Parasitol.* 31:336–345.

Krause, R.M., B. Buisson, S. Bertrand, P.J. Corringer, J.L. Galzi, J.P. Changeux, and D. Bertrand. 1998. Ivermectin: a positive allosteric effector of the α7 neuronal nicotinic acetylcholine receptor. *Mol. Pharmacol.* 53:283–294.

Krusek, J., and H. Zemková. 1994. Effect of ivermectin on γ-aminobutyric acid-induced chloride currents in mouse hippocampal embryonic neurones. *Eur. J. Pharmacol.* 259:121–128.

Lankas, G.R., M.E. Cartwright, and D. Umbenhauer. 1997. P-glycoprotein deficiency in a subpopulation of CF-1 mice enhances avermectin-induced neurotoxicity. *Toxicol. Appl. Pharmacol.* 143: 357–365.

McManus, O.B., and K.L. Magleby. 1988. Kinetic states and modes of single large-conductance calcium-activated potassium channels in cultured rat skeletal muscle. *J. Physiol.* 402:79–120.

McManus, O.B., and K.L. Magleby. 1991. Accounting for the Ca^{2+}-dependent kinetics of single large-conductance Ca^{2+}-activated K^+ channels in rat skeletal muscle. *J. Physiol.* 443:739–777.

Negulyaev, Y.A., and F. Markwardt. 2000. Block by extracellular Mg^{2+} of single human purinergic $P2X_4$ receptor channels expressed in human embryonic kidney cells. *Neurosci. Lett.* 279:165–168.

Nicke, A., H.G. Bäumert, J. Rettinger, A. Eichele, G. Lambrecht, E. Mutschler, and G. Schmalzing. 1998. $P2X_1$ and $P2X_3$ receptors form stable trimers: a novel structural motif of ligand-gated ion channels. *EMBO J.* 17:3016–3028.

Nobmann, S., B. Bauer, and G. Fricker. 2001. Ivermectin excretion by isolated functionally intact brain endothelial capillaries. *Br. J. Pharmacol.* 132:722–728.

North, R.A. 2002. Molecular physiology of P2X receptors. *Physiol. Rev.* 82:1013–1067.

Sakmann, B., and E. Neher. 1995. Single-Channel Recording, 2nd edition. Plenum Press, New York.

Shan, Q., J.L. Haddrill, and J.W. Lynch. 2001. Ivermectin, an unconventional agonist of the glycine receptor chloride channel. *J. Biol. Chem.* 276:12556–12564.

Sigel, E., and R. Baur. 1987. Effect of avermectin B_{1a} on chick neuronal γ-aminobutyrate receptor channels expressed in Xenopus oocytes. *Mol. Pharmacol.* 32:749–752.

Sigworth, F.J., and S.M. Sine. 1987. Data transformations for improved display and fitting of single-channel dwell time histograms. *Biophys. J.* 52:1047–1054.

Silberberg, S.D., and C. van Breemen. 1992. A potassium current activated by lemakalim and metabolic inhibition in rabbit mesenteric artery. *Pflugers Arch.* 420:118–120.

Stoop, R., S. Thomas, F. Rassendren, E. Kawashima, G. Buell, A. Surprenant, and R.A. North. 1999. Contribution of individual subunits to the multimeric $P2X_2$ receptor: estimates based on methanethiosulfonate block at T336C. *Mol. Pharmacol.* 56:973–981.

Vassilatis, D.K., J.P. Arena, R.H. Plasterk, H.A. Wilkinson, J.M. Schaeffer, D.F. Cully, and L.H. Van der Ploeg. 1997. Genetic and biochemical evidence for a novel avermectin-sensitive chloride channel in *Caenorhabditis elegans*. Isolation and characterization. *J. Biol. Chem.* 272:33167–33174.

Zheng, Y., B. Hirschberg, J. Yuan, A.P. Wang, D.C. Hunt, S.W. Ludmerer, D.M. Schmatz, and D.F. Cully. 2002. Identification of two novel *Drosophila melanogaster* histamine-gated chloride channel subunits expressed in the eye. *J. Biol. Chem.* 277:2000–2005.

Zufall, F., C. Franke, and H. Hatt. 1989. The insecticide avermectin B_{1a} activates a chloride channel in crayfish muscle membrane. *J. Exp. Biol.* 142:191–205.